Available online at www.sciencedirect.com
ScienceDirect
European Journal of Mechanics B/Fluids 26 (2007) 720–728

Free surface deformation due to a source or a sink in Stokes flow

Jae-Tack Jeong

School of Mechanical Systems Engineering, Chonnam National University, 300 Yongbong-Dong, Gwangju, 500-757, Korea

Received 11 September 2006; received in revised form 17 November 2006; accepted 15 February 2007

Available online 23 February 2007

Abstract

Free surface shape and cusp formation are analyzed by considering two-dimensional viscous flow due to a line source or a line sink below the free surface where the strength of source/sink is given arbitrarily. In the analysis, the Stokes' approximation is used and surface tension effects are included, but gravity is neglected. The solution is obtained analytically by using conformal mapping and complex function theory. From the solution, shapes of the free surface are shown and the formation of a cusp on the free surface is discussed. As the capillary number decreases in negative, the free surface shape becomes singular and in a real fluid a cusp should form on the free surface below some negative critical capillary number. Typically, streamline patterns for some capillary numbers are also shown. As the small capillary number vanishes, the solution is reduced to a linearized potential flow solution.

Keywords: Free surface; Source; Sink; Stokes flow; Cusp; Surface tension; Capillary number; Conformal mapping

1. Introduction

Some flow visualizations by photographs of free-surface flows of both Newtonian and non-Newtonian fluids at low Reynolds numbers have been carried out [1,2]. These photographs show compelling evidence for the formation of two-dimensional cusps on the free surface in the regions of convergence of the flow. The dynamical mechanism related to the cusp on the free surface in a Stokes flow has recently become a subject of theoretical and experimental researches. In the paper of Jeong and Moffatt [3] they carried out experiments using a pair of counter-rotating cylinders in a Newtonian fluid with free surface. For very slow rotation rates, there is a stagnation line on the free surface, and in some circumstances a small rounded crest can form in the neighborhood of this stagnation line. When the rotation rate is increased however, the surface dips downward, and simple visual observation indicates the presence of a very sharp cusp on the free surface. A complete analytical solution of a model problem of this experiments was also obtained, where the full nature of the flow and the detail of the cusp formation procedure were explained. In the model problem, they considered a Stokes flow induced by a vortex dipole below the otherwise undisturbed free surface, where direction of the vortex dipole was perpendicular to the free surface. Jeong [4] generalized this model problem to the case in which the orientation of the vortex dipole beneath the free surface is arbitrary. Antanovskii [5] generalized to the case in which the interfacial tension is variable, and Cummings [6] to the steady bubble solutions in dipole-driven Stokes flow.

E-mail address: jtjeong@chonnam.ac.kr.

0997-7546/$ – see front matter
doi:10.1016/j.euromechflu.2007.02.001

In the present paper, we consider a Stokes flow induced by a source or a sink instead of a vortex dipole below the otherwise undisturbed free surface, where the strength of source/sink to be arbitrary. As a low Reynolds number limit, the Stokes' approximation is used and the effect of surface tension is included, but gravity effects are neglected. The solution is obtained analytically by using conformal mapping and complex variable techniques. From the solution, the deformation of the free surface and the formation of a cusp on the free surface are discussed and some streamline patterns are shown.

2. The method of solution

2.1. Mathematical formulation

Consider the flow region shown in Fig. 1(a), where the undisturbed fluid occupies the half space $y < 0$. A line source of strength k (outward flowrate $2\pi k$) is located at $z(x + \mathrm{i}y) = -\mathrm{i}d$. When $k < 0$, the source may be considered as a sink. Since d is the only length scale in the problem, we may take $d = 1$ in what follows and the source singularity is then located at $z = -\mathrm{i}$. The free surface Γ is distorted by the resulting flow. Assume that the Reynolds number $\mathrm{Re} \equiv k/\nu$ is small so that the stream function Ψ satisfies the biharmonic equation $\nabla^4\Psi = 0$.

It is well known that Ψ can then be expressed in the form [7]

$$\Psi = \mathrm{Im}\big[f(z) + \bar{z}g(z)\big], \tag{1}$$

where the overbar represents the complex conjugate, and $f(z)$, $g(z)$ are two complex functions analytic at all points z in the fluid domain except at the source singularity at $z = -\mathrm{i}$,

$$f(z) \to k\ln(z + \mathrm{i}), \qquad g(z) \to \textit{finite}, \tag{2}$$

where the real constant k represents the strength of the source ($2\pi k$ is the flowrate of the source). The velocity components (u, v) are then given by

$$u - \mathrm{i}v = f'(z) + \bar{z}g'(z) - \overline{g(z)}, \tag{3}$$

and the pressure (p) and vorticity (Ω) fields are given by

$$p - \mathrm{i}\mu\Omega = 4\mu g'(z), \tag{4}$$

where μ is the viscosity. It is easy to verify that, with these relations, the Stokes equation $\nabla p = \mu\nabla^2\mathbf{u}$ is satisfied in the fluid.

As shown by Richardson [8], velocity and stress boundary conditions on the free surface Γ take the form

$$f'(z) + \bar{z}g'(z) - \overline{g(z)} = u_0(z)\overline{\left(\frac{\mathrm{d}z}{\mathrm{d}s}\right)}, \tag{5}$$

$$f'(z) + \bar{z}g'(z) + \overline{g(z)} = -\mathrm{i}\frac{\gamma}{2\mu}\overline{\left(\frac{\mathrm{d}z}{\mathrm{d}s}\right)}, \tag{6}$$

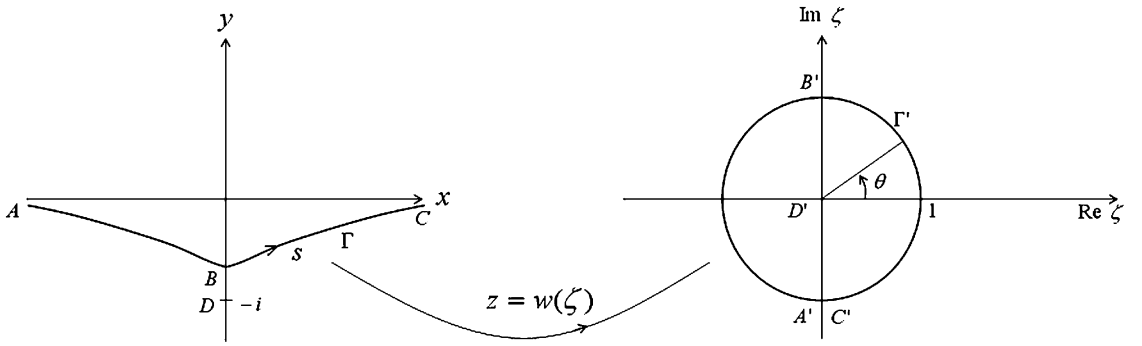

(a) z-plane (b) ζ-plane

Fig. 1. Free surface deformation with a source/sink and conformal mapping into the unit circle.

where s is the arclength on Γ measured from the point of symmetry B (Fig. 1(a)), γ the surface tension coefficient, and $u_0(z)$ the real tangential velocity at an arbitrary point z on the free surface. The manipulation of (5) and (6) yields the following equations (for $z \in \Gamma$)

$$f(z) + \bar{z}g(z) = 0, \tag{7}$$

$$\mathrm{Im}\left[\overline{\left(\frac{\mathrm{d}z}{\mathrm{d}s}\right)}g(z)\right] = \frac{\gamma}{4\mu}. \tag{8}$$

The conditions $u, v \to 0$ at infinity ($|z| \to \infty$) are satisfied provided

$$f(z) \to cz, \quad g(z) \to \bar{c}, \quad \text{as } |z| \to \infty, \tag{9}$$

where c is an arbitrary constant. We can find from (5) and (6) that the choice $c = -\mathrm{i}\gamma/4\mu$ is appropriate. Eqs. (2) and (5)–(9) constitute the essential boundary conditions that $f(z)$ and $g(z)$ must satisfy. The symmetry conditions $\Psi = 0$, $\Omega = 0$ on $x = 0$ clearly imply that

$$\mathrm{Im}\{f(\mathrm{i}y)\} = 0, \quad \mathrm{Re}\{g(\mathrm{i}y)\} = 0. \tag{10}$$

Since this problem is similar to that of Jeong and Moffatt [3] except the source/sink singularity boundary condition (2) at $z = -\mathrm{i}$, we may follow the same procedure as in Ref. [3].

2.2. Conformal mapping

Let $z = w(\zeta)$, yet unknown, be the conformal mapping that maps the fluid domain D onto the unit disk $D' : |\zeta| \leqslant 1$, and which places the (imaged) source at $\zeta = 0$, so that $w(0) = -\mathrm{i}$ (Fig. 1(b)). The points A, B, C, D of Fig. 1(a) map to the points A', B', C', D' of Fig. 1(b), respectively. Let

$$F(\zeta) \equiv f\{w(\zeta)\} = f(z), \tag{11}$$

$$G(\zeta) \equiv g\{w(\zeta)\} = g(z), \tag{12}$$

$$U(\zeta) \equiv u_0\{w(\zeta)\} = u_0(z), \tag{13}$$

so that

$$f'(z) = \frac{F'(\zeta)}{w'(\zeta)}, \qquad g'(z) = \frac{G'(\zeta)}{w'(\zeta)}. \tag{14}$$

By the conformal mapping property, it follows that, for $z \in \Gamma$, i.e. $|\zeta| = 1$,

$$\frac{\mathrm{d}z}{\mathrm{d}s} = -\mathrm{i}\zeta\frac{w'(\zeta)}{|w'(\zeta)|}, \tag{15}$$

$$\overline{\left(\frac{\mathrm{d}z}{\mathrm{d}s}\right)} = \frac{\mathrm{i}}{\zeta}\frac{\overline{w'(\zeta)}}{|w'(\zeta)|}. \tag{16}$$

Hence boundary conditions (5) and (6) become, on $|\zeta| = 1$,

$$\frac{F'(\zeta)}{w'(\zeta)} + \overline{w(\zeta)}\frac{G'(\zeta)}{w'(\zeta)} - \overline{G(\zeta)} = U(\zeta)\frac{\mathrm{i}}{\zeta}\frac{\overline{w'(\zeta)}}{|w'(\zeta)|}, \tag{17}$$

and

$$\frac{F'(\zeta)}{w'(\zeta)} + \overline{w(\zeta)}\frac{G'(\zeta)}{w'(\zeta)} + \overline{G(\zeta)} = \frac{\gamma}{2\mu\zeta}\frac{\overline{w'(\zeta)}}{|w'(\zeta)|}. \tag{18}$$

Subtracting (17) from (18) and taking the complex conjugate gives

$$\frac{G(\zeta)}{\zeta w'(\zeta)} = \frac{1}{2|w'(\zeta)|}\left(\frac{\gamma}{2\mu} + iU(\zeta)\right), \quad \text{on } |\zeta| = 1. \tag{19}$$

Since $w(\zeta)$ is a conformal mapping function, $w'(\zeta)$ is analytic and non-zero in $|\zeta| < 1$, and the left-hand side of (19) is analytic in $|\zeta| < 1$ except a simple pole at $\zeta = 0$. To remove this singularity, we subtract $G(0)/\zeta w'(0)$ from each side of (19):

$$\frac{G(\zeta)}{\zeta w'(\zeta)} - \frac{G(0)}{\zeta w'(0)} = \frac{1}{2|w'(\zeta)|}\left(\frac{\gamma}{2\mu} + \mathrm{i}U(\zeta)\right) - \frac{G(0)}{\zeta w'(0)} \quad \text{on } |\zeta| = 1. \tag{20}$$

Now, the left-hand side of (20) is the boundary value of a function analytic in $|\zeta| < 1$. If $w(\zeta)$ and $G(0)$ can be found, then the real part of the right-hand side of (20) will be known, so that $G(\zeta)$ may be found [7]. From the symmetry condition (10), we can see $G(0)$ is pure imaginary and $w'(0)$ is real. Hence, the formal expression of $G(\zeta)$ is, for $|\zeta| \leqslant 1$,

$$\frac{G(\zeta)}{\zeta w'(\zeta)} = \frac{G(0)}{w'(0)}\left(\zeta + \frac{1}{\zeta}\right) + \frac{1}{2\pi\mathrm{i}} \oint\limits_{|\zeta_0|=1} \frac{\gamma}{4\mu|w'(\zeta_0)|} \frac{\zeta_0 + \zeta}{\zeta_0(\zeta_0 - \zeta)}\,\mathrm{d}\zeta_0, \tag{21}$$

where $w'(\zeta)$ and $G(0)$ should be determined. To consider the behavior of this expression as $|\zeta| \to 1$, we put $\zeta_0 = \mathrm{e}^{\mathrm{i}\theta_0}$ and $\zeta = \mathrm{e}^{\mathrm{i}\theta}$ in (21), then

$$\frac{G(\zeta)}{\zeta w'(\zeta)} = 2\cos\theta \frac{G(0)}{w'(0)} + \frac{\gamma}{4\mu|w'(\zeta)|} + \frac{\mathrm{i}\gamma}{8\pi\mu} \int\limits_0^{2\pi} \frac{1}{|w'(\mathrm{e}^{\mathrm{i}\theta_0})|} \frac{\cos\theta + \cos\theta_0}{\sin\theta - \sin\theta_0}\,\mathrm{d}\theta_0, \tag{22}$$

where the principal value is used for integral. Recalling that $G(0)$ is pure imaginary from (10), we see that the real part of this expression is $\gamma/4\mu|w'(\zeta)|$ as required by (19).

Now, consider that the boundary conditions (2), (7) transform in the ζ plane to

$$F(\zeta) \to k\ln\zeta, \quad \text{as } \zeta \to 0, \tag{23}$$

$$F(\zeta) = -\overline{w(\zeta)}G(\zeta) = -w^*(\zeta)G(\zeta) \quad \text{on } |\zeta| = 1, \tag{24}$$

since $\bar{\zeta} = 1/\zeta$ on $|\zeta| = 1$. The function w^* in (24) is defined as $w^*(\zeta) = \overline{w(1/\bar{\zeta})}$. Note that the boundary condition (23) has a logarithmic singularity at $\zeta = 0$, which is somewhat difficult to be satisfied. However, considering bilinear transformation and observing the boundary conditions (23) and (24) carefully, we have found an appropriate integral form of the mapping function as

$$w(\zeta) = \int\limits_0^1 \mathrm{i}b(t)\frac{\zeta}{\zeta t + \mathrm{i}}\,\mathrm{d}t + \mathrm{i}\frac{\zeta - \mathrm{i}}{\zeta + \mathrm{i}}, \tag{25}$$

where $b(t)$ in $0 \leqslant t \leqslant 1$ is a real function to be determined. Then $w(0) = -\mathrm{i}$ is satisfied and the conjugate function $w^*(\zeta)$ becomes

$$w^*(\zeta) = -\int\limits_0^1 \frac{\mathrm{i}b(t)}{t - \mathrm{i}\zeta}\,\mathrm{d}t + \mathrm{i}\frac{\zeta - \mathrm{i}}{\zeta + \mathrm{i}}. \tag{26}$$

Note that the mapping function $w(\zeta)$ in (25) is analytic in $|\zeta| < 1$ whereas $w^*(\zeta)$ in (26) is analytic in $|\zeta| > 1$. By introducing $w(\zeta)$ in the form (25), the logarithmically singular boundary condition (23) can be satisfied, as will be seen later. Substituting (26) into (24), we get $F(\zeta)$ in $|\zeta| \leqslant 1$, by applying Cauchy's integral theorem [7],

$$F(\zeta) = -w^*(\zeta)G(\zeta) = \left\{\int\limits_0^1 \frac{\mathrm{i}b(t)}{t - \mathrm{i}\zeta}\,\mathrm{d}t - \mathrm{i}\frac{\zeta - \mathrm{i}}{\zeta + \mathrm{i}}\right\}G(\zeta). \tag{27}$$

Since the stream function (1) must be discontinuous due to the source flow of strength k, $F(\zeta)$ in (27) should have discontinuity $2\pi\mathrm{i}k$ across the line between $\zeta = 0$ and $-\mathrm{i}$. Therefore,

$$G(-\mathrm{i}t_0) = \frac{k\mathrm{i}}{b(t_0)} \quad \text{for } 0 \leqslant t_0 \leqslant 1. \tag{28}$$

Substituting $\zeta = -\mathrm{i}t_0$ $(0 \leqslant t_0 < 1)$ in (21) and using (28), we get

$$-\frac{k}{t_0 b(t_0) w'(-\mathrm{i}t_0)} = \frac{k}{b(0)w'(0)}\left(t_0 - \frac{1}{t_0}\right) + \frac{1}{2\pi\mathrm{i}} \oint\limits_{|\zeta_0|=1} \frac{\gamma}{4\mu|w'(\zeta_0)|} \frac{\zeta_0 - \mathrm{i}t_0}{\zeta_0(\zeta_0 + \mathrm{i}t_0)}\,\mathrm{d}\zeta_0, \tag{29}$$

where the derivative $w'(\zeta)$ is expressed as

$$w'(\zeta) = \frac{\mathrm{d}w(\zeta)}{\mathrm{d}\zeta} = -\int\limits_0^1 \frac{b(t)}{(\zeta t + \mathrm{i})^2}\,\mathrm{d}t - \frac{2}{(\zeta + \mathrm{i})^2}. \tag{30}$$

Now, when we compare the imaginary parts of (19) and (22), we obtain an expression for the tangential free-surface velocity:

$$u_0(z) = U(\zeta) = U\left(\mathrm{e}^{\mathrm{i}\theta}\right) = -\cos\theta\left|w'\left(\mathrm{e}^{\mathrm{i}\theta}\right)\right|\left[\frac{4G(0)}{w'(0)}\mathrm{i} + \frac{\gamma}{4\pi\mu}\int\limits_0^{2\pi} \frac{\mathrm{d}\theta_0}{|w'(\mathrm{e}^{\mathrm{i}\theta_0})|(\sin\theta_0 - \sin\theta)}\right]. \tag{31}$$

From the condition that $u_0(z) \to 0$ as $|z| \to \infty$ (i.e. as $\theta \to -\pi/2$ in (31)), the term in square bracket in (31) must vanish as $\theta \to -\pi/2$, i.e.

$$G(0) = \frac{k\mathrm{i}}{b(0)} = \frac{\mathrm{i}\gamma w'(0)}{16\pi\mu}\int\limits_0^{2\pi} \frac{\mathrm{d}\theta_0}{|w'(\mathrm{e}^{\mathrm{i}\theta_0})|(\sin\theta_0 + 1)}. \tag{32}$$

Combining (29), (32) and canceling $b(0)$, we obtain the relation as

$$\frac{1}{b(t_0)} = \frac{1}{16\pi Ca} w'(-\mathrm{i}t_0)\left(1 - t_0^2\right)(1 - t_0)^2 \int\limits_0^{2\pi} \frac{\mathrm{d}\theta_0}{|w'(\mathrm{e}^{\mathrm{i}\theta_0})|(\sin\theta_0 + 1)(2t_0\sin\theta_0 + 1 + t_0^2)}, \tag{33}$$

for $0 \leqslant t_0 < 1$, where the capillary number Ca is defined as

$$Ca \equiv \frac{\mu k}{\gamma d}. \tag{34}$$

Eq. (33) is a kind of non-linear integral equation [9] for $b(t_0)$ since the function w' in (33) involves $b(t_0)$ as (30). In the limit of $t_0 \to 1$, (33) gives $b(t_0) \to 4Ca$, which is consistent with $G(\zeta) \to \mathrm{i}\gamma/4\mu$ as $\zeta \to -\mathrm{i}$ from boundary condition (9). Solving the integral equation (33) for $b(t_0)$ numerically, we obtain $b(t)$ in $0 \leqslant t \leqslant 1$ for a given capillary number Ca (i.e., for a given strength of the source). With $b(t)$ $(0 \leqslant t \leqslant 1)$ obtained, we derive $G(\zeta)$ in $|\zeta| \leqslant 1$ from (21) as

$$G(\zeta) = -\frac{k}{32\pi Ca} w'(\zeta)\left(\zeta + \frac{1}{\zeta}\right)(\zeta + \mathrm{i})^2 I\left(\zeta; b(t)\right), \tag{35}$$

where

$$I\left(\zeta; b(t)\right) \equiv \int\limits_0^{2\pi} \frac{\mathrm{d}\theta_0}{|w'(\mathrm{e}^{\mathrm{i}\theta_0})|(1 + \sin\theta_0)(\sin\theta_0 - (\zeta - \zeta^{-1})/2\mathrm{i})}. \tag{36}$$

Therefore, two complex functions $F(\zeta)$ and $G(\zeta)$ in the ζ-plane are obtained as (27) and (35), and hence $f(z)$ and $g(z)$ in the z-plane, which describe the whole solution of our flow due to the source.

3. Results

The real function $b(t)$ in the integral equation (33) can be determined for given complex capillary number Ca defined in (34). Numerical calculations for $b(t)$ are carried out by the iterative method with initial guess $b(t) = b(1) = 4Ca$ for $0 \leqslant t < 1$. Graphs of $b(t)$ are shown for some values of Ca in Fig. 2. For $Ca < -0.43$, numerical

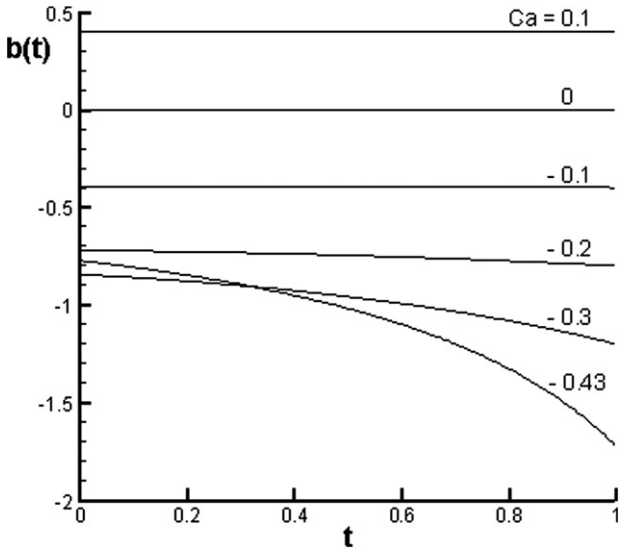

Fig. 2. Graphs of $b(t)$ in the mapping function $w(\zeta)$ in (25) for some capillary numbers Ca.

calculation becomes hard to get a converged solution since the integrand in (33) becomes steep around $\theta_0 = \pi/2$. Using $b(t)$ determined in this way, we can obtain free surface shape and streamlines for some values of capillary number Ca.

3.1. Free surface

The free surface Γ is given by $z = x + \mathrm{i}y = w(\zeta)$ with $\zeta = \mathrm{e}^{\mathrm{i}\theta}$, or, from (25),

$$x(\theta) = \left\{ \int_0^1 \frac{b(t)}{t^2 + 2t\sin\theta + 1}\,\mathrm{d}t + \frac{1}{1+\sin\theta} \right\} \cos\theta, \tag{37a}$$

$$y(\theta) = \int_0^1 \frac{b(t)(t+\sin\theta)}{t^2 + 2t\sin\theta + 1}\,\mathrm{d}t. \tag{37b}$$

The free surface shapes are shown in Fig. 3 for some values of capillary number Ca. For some sufficiently lower values of Ca than $Ca = -0.43$, a cusp is likely to occur at $x = 0$ on the free surface. As $Ca \to -\infty$, a genuine cusp would occur. In that case, the mapping at the cusp point is not conformal and $w'(i)$ must be zero, hence the integral equation (33) becomes singular. Near the cusp point, as explained by Jeong and Moffatt [3] and Jeong [4], the characteristic length scale reaches to the molecular scale and the continuum hypothesis fails hence the effects of intermolecular forces should be considered. Eggers [10] insisted that the air (second fluid outside) drawn into the cusp entered the fluid destroying the cusp solution and the molecular scales were never reached.

At $\theta \to -\pi/2$ in (37), we can see

$$x(\theta) \to \frac{2}{\theta + \pi/2}, \qquad y(\theta) \to b(1) \ln\left|\theta + \frac{\pi}{2}\right|, \tag{38}$$

hence

$$y \to -4Ca \ln|x| \quad \text{as } x \to \pm\infty. \tag{39}$$

This provides an interesting result that the free surface far from the source (or sink) falls down (or grows up) logarithmically.

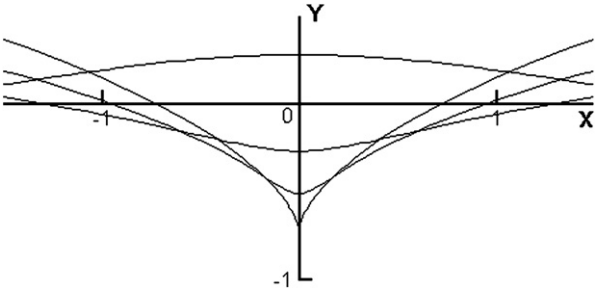

Fig. 3. Free surface shapes for some values of Ca.

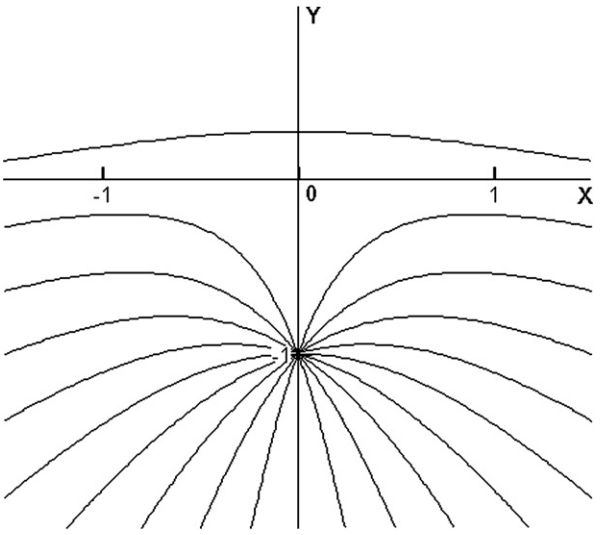

Fig. 4. Streamline pattern for $Ca = 0.1$. Here $\Delta\Psi/2\pi k = 0.05$.

In the limit of $Ca\ (= \mu k/\gamma) \to 0$, (33) is reduced to $b(t) \to 4Ca$, hence $y = \mathrm{O}(Ca)$ from (37b). This means that, for very large surface tension or very weak strength of source/sink, deformation of the free surface is very small and free surface shape tends to be horizontal. Moreover, from (37), we can obtain

$$y \approx -2Ca \ln\left(\frac{x^2+1}{4}\right), \quad \text{for } |Ca| \ll 1, \tag{40}$$

which agrees with a linearized result of our problem and confirms (39).

3.2. Stream function and flow patterns

Substituting $F(\zeta)$, $G(\zeta)$ obtained from (27), (35) into (1), we get a stream function

$$\Psi = (1-\zeta\bar{\zeta})\mathrm{Im}\left[G(\zeta)\left\{\int_0^1 \frac{b(t)}{(t-\mathrm{i}\zeta)(\bar{\zeta}t-\mathrm{i})}\,\mathrm{d}t + \frac{2\mathrm{i}}{|\zeta+\mathrm{i}|^2}\right\}\right]. \tag{41}$$

For some values of $Ca = 0.1, 0, -0.2, -0.43$, the flow patterns are shown in Figs. 4–7.

Additionally, the tangential velocity $u_0(z)$ on the free surface Γ may also be derived from (31) and (32) by

$$u_0(z) = U\left(\mathrm{e}^{\mathrm{i}\theta}\right) = -\frac{k}{4\pi Ca}(1+\sin\theta)\cos\theta\left|w'\left(\mathrm{e}^{\mathrm{i}\theta}\right)\right|\left[\int_0^{2\pi} \frac{\mathrm{d}\theta_0}{|w'(\mathrm{e}^{\mathrm{i}\theta_0})|(\sin\theta_0+1)(\sin\theta_0-\sin\theta)}\right], \tag{42}$$

where the principal value is used for the integral. With θ related to x by (37a), (42) determines u_0/k implicitly as a function of x. This function is shown in Fig. 8 for various values of Ca. The curve corresponding to $Ca = 0$ coincides with that obtained by a linearized analysis. The free surface velocity is directed towards or away from the stagnation point on the free surface according as $Ca < 0$ or $Ca > 0$.

For the limiting case of the capillary number $Ca \to 0$,

$$w'(\zeta) \to \frac{-2}{(\zeta+\mathrm{i})^2}, \quad b(t) \to 4Ca, \quad G(\zeta) \to \frac{i\gamma}{4\mu}.$$

Hence the stream function Ψ in (41) becomes

$$\Psi \to -k\mathrm{Im}\left[\ln\left\{\frac{\zeta+\mathrm{i}}{\mathrm{i}\zeta(\bar{\zeta}-\mathrm{i})}\right\}\right] \to k\mathrm{Im}\left\{\ln\left(z^2+1\right)\right\},$$

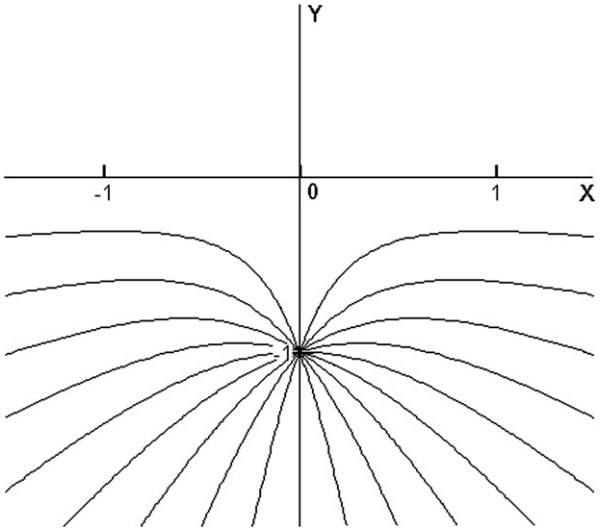

Fig. 5. Streamline pattern for $Ca = 0$. The results are exactly the potential flow solution. Here $\Delta\Psi/2\pi k = 0.05$.

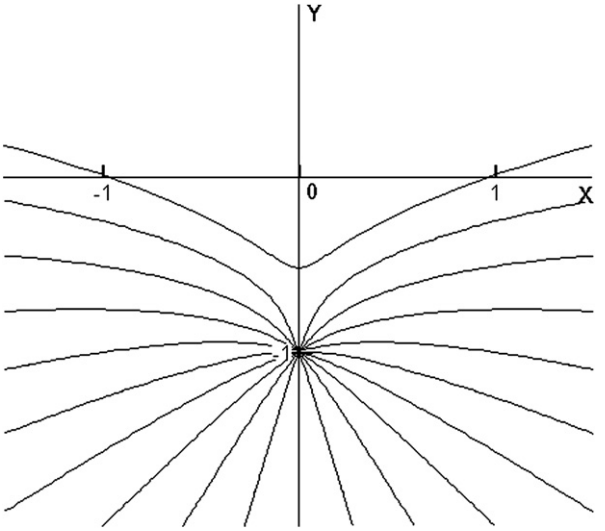

Fig. 6. Streamline pattern for $Ca = -0.2$. Here $\Delta\Psi/2\pi k = 0.05$.

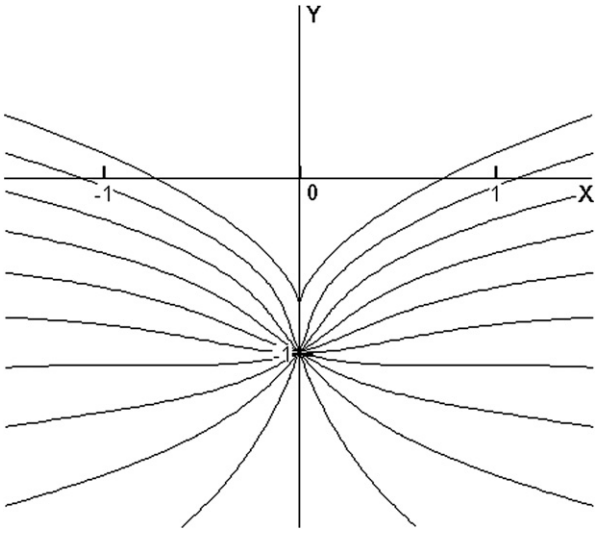

Fig. 7. Streamline pattern for $Ca = -0.43$. Here $\Delta\Psi/2\pi k = 0.05$.

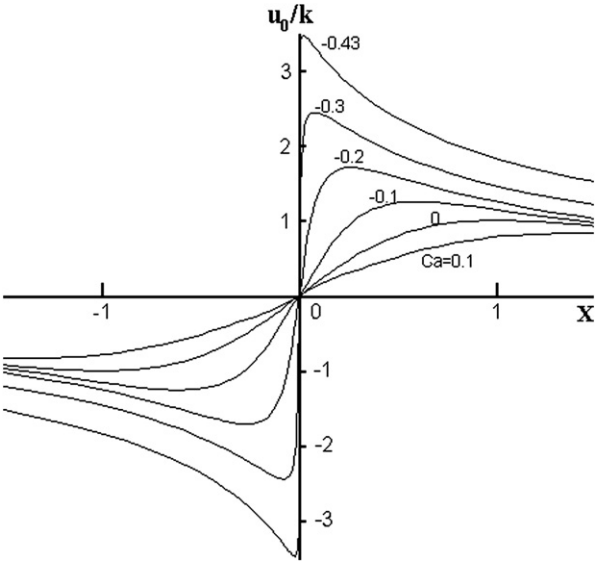

Fig. 8. Tangential velocity $u_0(x)$ on Γ normalized with respect to the strength k of the source.

and the tangential free-surface velocity $u_0(z)$ in (42) becomes

$$u_0(z) \to k\cos\theta \to \frac{2kx}{x^2+1},$$

which are well-known results of the linearized potential flow solution.

4. Conclusion

In this paper, Stokes flow due to a source or a sink below the free surface where the strength of source/sink is given arbitrarily is solved analytically by using the complex function theory. While the gravity is neglected in this model, we have obtained many valuable insights into the formation of cusp on the free surface. Actually, near the cusp, surface

tension effects are dominant to the gravitational effects. For arbitrary strength of source/sink, the whole flow fields are determined including the shape of free surface and the velocity on the free surface. We conclude that the cusp occurs on the free surface for sufficiently large capillary number Ca. As the capillary number vanishes, our solution tends to the well-known potential flow solution, as expected. Much further theoretical research may also be motivated by considering the effects neglected in this analysis, such as air (second fluid outside) near the cusp, unsteadiness, variable surface tension, the gravity effects, and so on.

Acknowledgement

This work was supported by the Korea Research Foundation Grant funded by the Korean Government (MOEHRD) (KRF-2004-002-D00070).

References

[1] D.D. Joseph, J. Nelson, M. Renardy, Y. Renardy, Two-dimensional cusped interfaces, J. Fluid Mech. 223 (1991) 383.
[2] Y.J. Liu, T.Y. Liao, D.D. Joseph, A two dimensional cusp at the trailing edge of an air bubble rising in a viscoelastic liquid, J. Fluid Mech. 304 (1995) 321.
[3] J.-T. Jeong, H.K. Moffatt, Free-surface cusps associated with flow at low Reynolds number, J. Fluid Mech. 241 (1992) 1.
[4] J.-T. Jeong, Formation of cusp on the free surface at low Reynolds number flow, Phys. Fluids 11 (1999) 521.
[5] L.K. Antanovskii, Influence of surfactants on a creeping free boundary flow induced by two counter-rotating horizontal thin cylinders, Eur. J. Mech. B Fluids 13 (1994) 73.
[6] L.J. Cummings, Steady solutions for bubbles in dipole-driven Stokes flows, Phys. Fluids 12 (2000) 2162.
[7] N.I. Muskhelishvili, Some Basic Problems of the Mathematical Theory of Elasticity, third ed., P. Noordhoff, 1953.
[8] S. Richardson, Two dimensional bubbles in slow viscous flows, J. Fluid Mech. 33 (1968) 475.
[9] F.G. Tricomi, Integral Equations, fourth ed., John Wiley & Sons, 1967, pp. 197–213.
[10] J. Eggers, Air entrainment through free-surface cusp, Phys. Rev. Lett. 86 (2001) 4290.